Electronic Supplementary Material (ESI) for Analyst.

The Applications and Methodologies of Mass Spectrometry Imaging in Plants, Microbes, and Food: A Review

Mudita Vats[a], Berta Cillero-Pastor[a,b], Eva Cuypers[a] and Ron M.A. Heeren[a*]

[a] Maastricht MultiModal Molecular Imaging Institute (M4i), Division of Imaging Mass Spectrometry, Maastricht University, Maastricht, the Netherlands
[b]MERLN Institute for Technology-inspired Regenerative Medicine, Department of Cell Biology-Inspired Tissue Engineering (cBITE), Maastricht University, Maastricht, the Netherlands

* Corresponding author's contact details: Prof. Dr. Ron M.A. Heeren, The Maastricht MultiModal Molecular Imaging (M4I) institute, Division of Imaging Mass Spectrometry (IMS), Maastricht University, Maastricht, 6229 ER, Netherlands.
Telephone +31433881499, fax +31433884154, **r.heeren@maastrichtuniversity.nl**

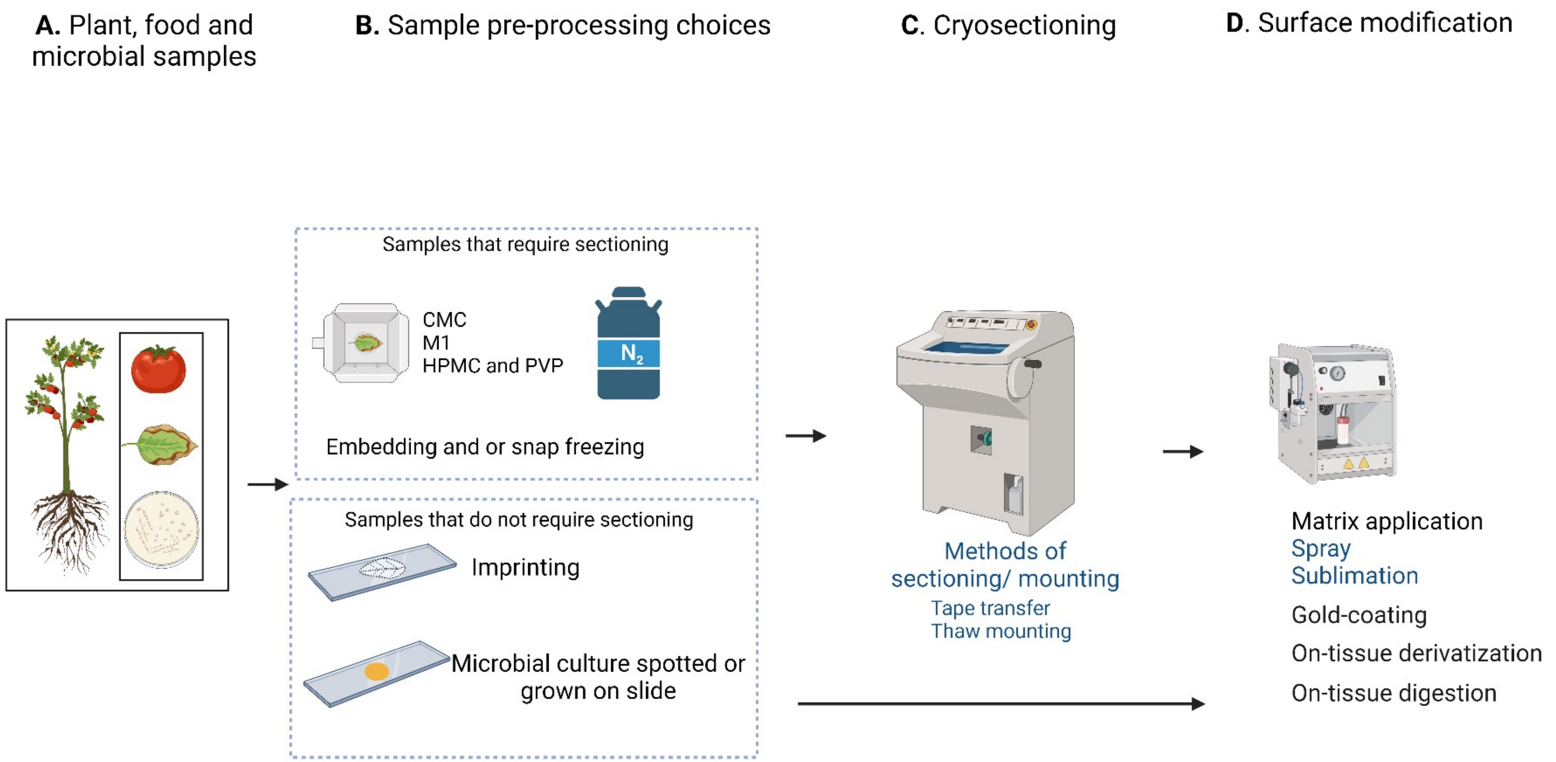

Figure S1: Sample preparation methods of plant, food and microbial samples. (A)The samples, (B) sample pre-processing is divided into two parts; samples that require sectioning (**snap freezing** or **embedding followed by snap freezing)** and the samples that do not need to section (**imprinting** or **culturing**). Most common embedding mediums include Carboxymethyl cellulose (CMC), M1 embedding medium and mixture of hydroxypropyl methylcellulose (HPMC) and polyvinylpyrrolidone (PVP). (C) cryosectioning where the samples can be obtained by thaw mounting on the slides or with tape transfer method[1-3] and (D) the samples can then be further modified by application of matrix, gold-coating, on-tissue derivatization or on-tissue tryptic digestion depending on the requirement of the research. Figure Created with BioRender.com

Table 1 *Literature review of sample types, analytical techniques used, project objectives, compound types, and spatial resolutions in the reviewed studies*

Sample	**Technique**	**Project purpose**	**Compound types**	**Spatial resolution**	**Reference**
Plant root-bacteria	MALDI-MSI and ESI-Q-TOF	Metabolite distribution in roots and root nodules of *M. truncatula* during nitrogen fixation.	Organic acids, amino acids, sugars, lipids and flavonoids	Spot diameter 50 µm	4
Strawberry	MALDI-MSI and MALDI-MS	MALDI-MSI analysis for food-related metabolites in ripe strawberries	Anthocyanin, sugars and organic acids	Step size 200µm	5
Blueberry	MALDI-FT-ICR-MSI, UHPLC-HRMS, ICS	Understand the spatial accumulation patterns of polyphenols and related primary metabolites during bilberry fruit development	Secondary metabolites (flavonoids and HCAs) and related primary metabolites (sugars and amino acids)	laser beam width ~30 µm, raster step size of 60 µm	6
Soybean-aphid and rice-bacteria	MALDI and NALDI	Plant-pest interactions in soybean-aphid and rice-bacteria	Pipecolic acid, salicylic acid, phytoalexins, momilactones, phytocassanes, nucleobases, phosphocholine and amino acids	30µm and 10µm	7
Tomato	MALDI, LC-MS	Metabolites associated to ripening and physical stress	Malate, aspartate, glutamine, caffeate and AMP	50 µm	8

Leaves of G. sepium	MALDI-MSI, LDI-MS, LDI-MSI, ESI-MS	Plant's cosmetic potential	Polyphenol, fatty acids and flavonoids	30µm	9
Leaves of coca	MALDI-FT-ICR-MSI, LDI-MS, ESI-MS	Distribution of alkaloids	Cocaine	50 µm × 50 to 160 µm × 160 µm	10
Streptomyces coelicolor	ToF-SIMS	Distribution of two antibiotics in *Streptomyces coelicolor*	Blue antibiotic (major constituent actinorhodin) Red antibiotic (major constituents-butylcycloheptylprodiginine and undecylprodigiosin)	not mentioned	11
Bacteria and fungal hyphae	ToF-SIMS	Carbon (C) and nitrogen (N) assimilation by individual bacterium and fungal hyphae in soil		<200 nm	12
Prunus laurocerasus	ToF-SIMS	Distribution of herbicides on the cuticle of leaves of *Prunus laurocerasus* and the diffusion into the sub-surface	Surfactants and sulfosates	1 µm	13
Bacillus amyloliquefaciens S499 associated with tomato	ToF-SIMS and LC-ESI-MS	Study the in-situ production of a class of antibiotics by *Bacillus amyloliquefaciens S499* in the roots of tomato	Cyclic lipopeptides	not mentioned	14
Populous tremuloides	ToF-SIMS and SEM	Distributions of heavy metals in rhizospheric region of *populous tremuloides*	Calcium (Ca), magnesium (Mg), sodium (Na), potassium (K), silicon (Si) and aluminium (Al)	1.5 µm	15

Plant root-microorganisms	Nano-SIMS and TEM	Visualize the distribution of $^{15}N/^{14}N$ in-situ in symbiotic relationship	$^{15}N/^{14}N$	100 nm	[16]
Anabaena and rhizobium	Nano-SIMS and EL-FISH	Mutualistic interaction of filamentous *Anabaena* and Rhizobium	Isotopically labelled carbon and nitrogen	~ 150 nm	[17]
Ivy and jade plant	SF-PESI-MS and LESA-MS	Pesticides on plant parts	Pesticide formulation (acephate)	na	[18]
Schizophyllum commune and *Hypholoma fasciculare*	LESA-HRMS and Raman microscopy	Study the metabolic interactions between two wood-rot fungi, *Schizophyllum commune* and *Hypholoma fasciculare*	Secondary metabolites such as indigo, indirubin and isatin		[19]
Rice node	LA-ICP-MSI	Localization of macro and micro-elements in rice	Mg, Ca, K, Cu, Mn and Fe	8 to 25 µm	[20]
Sunflower leaves	LA-ICP-MSI	Localization of macro and micro-elements in sunflower leaves	Ca, Cr, P, Fe, S, Cd, Ce, Cu, La, Mn, K, Ni and Zn	180 µm	[21]
Coptis chinensis Franch	LA-ICP-MSI	Spatial micromapping of Cr and other elements in Coptis chinensis Franch	Cr, Fe, Mn, Ca, and Zn	spot diameter 44 µm	[22]
Arabidopsis thaliana and *hypericum perforatum*	LDI-MSI	Localize UV-absorbing secondary metabolites in single cells of Arabidopsis thaliana and hypericum perforatum	Hypercin, pseudohypercin, quercetin, rutin, kaempferol, isorhamnetin	~10 µm	[23]
Vitis vinifera leaves	LDI-MSI and fluorescence microscopy	The spatial distributions of viniferins in UV-stressed and *plasmopara viticola* infected *vitis vinifera*	Phytoalexins, stilbene, viniferins	50 µm	[24]
Allium cepa and Fittonia argyroneura	LAESI-MSI	Metabolite content in individual *Allium cepa* cells and *Fittonia argyroneura* leaves	Malic acid , maleic acid, catechol, furoic acid, phthalide, and glycineamideribonucleotide		[25]
Allium cepa	LAESI-MSI	Distinguish between pigmented and non-pigmented cells of onion (*Allium cepa*)	Cyanidin	~ 30 µm	[26]

Lemon, rose, rye, cherry tomato, and maize	LAESI-MSI	Pesticide residues on plant surfaces	Imazalil, thiabendazole, lycoperoside and esculeoside	150 µm	27
Grape vine	DESI-MSI	Distribution of metabolites in grapevine stem	Malic acid, tartaric acid, citric acid, glutaric acid and adipic acid	200 µm step size	28
Grapes, wine and fabric	Nano-DESI-MSI	Detect the presence of anthocyanin in wine and grapes from different cultivars	Anthocyanin		29
Potato	DESI-MSI	Metabolic changes during *Pythium ultimum* infection in potatoes	Glycoalkaloids, solasodiene, solanidine, solasodenone, solasodine, solanaviol, and solaspiralide	Lateral spatial resolution150 to 200 µm	30
Bacteria, fungi and oomycetes	DESI-MSI	Interactions between endophytic bacteria and cacao pathogen	Metabolites and phospholipids such as Pyrrolnitrin glycerophosphoethanolamines, glycerophosphatidic acid, and glycerophosphoglycerols	spatial resolution of 200 µm	31
S. miltiorrhiza and *S. grandifolia*	DESI-MSI	Molecular mechanisms of terpenoid biosynthesis in *S. miltiorrhiza* and *S. grandifolia*	Tricyclic diterpenes like 11-hydroxy-sugiol, 11-hydroxy-ferruginol, 11,20-dihydroxy-sugiol, and 11,20-dihydroxy-ferruginol		32
Plant leaves	DESI-MSI	Investigation of pesticide distribution both on the surface of leaves and in cross sections of plant stem	Pyrethrins, rapeseed oil, imidacloprid and methiocarb	50-100 µm	33

Apple	3D-imaging with REIMS	Distinguish between molecular distributions on the apple peel and inside	Lipids	2 mm	[34]
Kiwi, orange, purple carrots, german sausage, gouda cheese and ginger bread	MALDI-MSI with AP-SMALDI10 ion source	Detect and image the ingredients, constituents, contaminants and additives in food	Anthocyanin, beta-carotene, natamycin, fat and acrylamide	Kiwi- 45 µm, carrot-50 µm, sausage- 20 µm, gingerbread-200 µm, cheese-20 µm	[35]
San Pedro cactus (Echinopsis pachanoi), jimsonweed (Datura stramonium) fruits and seeds, and tobacco (Nicotiana tabacum) seedlings	LDI	Distribution of plant metabolites in native tissues	Alkaloids, mescaline and nicotine	100 µm	[36]
Strawberry	MALDI-TOF-MSI	Distribution of strawberry plant metabolites at different maturity stages	Sugars, anthocyanin, phytochemicals	200µm	[37]
Kidney bean	MALDI-MSI	Derivatization of abscisic acid and 12-oxo-phytodienoic acid using GirT derivatization	Abscisic acid and 12-oxo-phytodienoic acid	100 µm	[38]
Cucumber	MALDI-FTICR-MSI	Distribution of procymidone in cucumber	Procymidone	100 µm	[39]
Sorghum	MALDI-MSI and LC-MS	accumulation of dhurrin (cyanogenic glucoside) in germinating sorghum	Metabolites, dhurrin and its recycling products	30 µm	[40]
Wheat grain	MALDI-MSI	Spatial distribution of polysaccharides in wheat endosperm	oligosaccharides	100 µm	[41]

Maize	AP-SMALDI-MSI	Spatial distribution of aflatoxin B1 and plant defense metabolites in maize	Furanocoumarin, chlorins, flavonoid glycosides, steroid lactones, carbohydrates and glycosyldiacylglycerols	≥5 µm laser spot size	42
Grape wine leaf	MALDI-FTICR	Spatial distribution of compounds during fungal infection	Stilbene phytoalexins	50 µm	43
Mung bean	MALDI	Lipids during germination	Glycerophospholipids, Glycerolipids, Sphingolipids and sterols	50 µm	44
Rhizome of *Glycyrrhiza uralensis* (licorice)	DESI-MSI	Distribution of small metabolites and oligosaccharides in the rhizome.	Small metabolites, flavonoids, isoflavones, triterpenoids and hydrolyzed oligosaccharides	200 µm	45
Cannabis leaves	DESI and MALDI MSI	Distribution of cannabinoids and flavonoids on the trichomes of leaves	Cannabinoids and flavonoids	DESI: 150-200 µm and MALDI-MSI: 20 µm	1
Tomato	MALDI-MSI, LC-MS	Function of Gorky compounds in tomato	Esculeoside, tomatine and acetoxytomatine	50 µm	3
Coffee	AP-MALDI-MSI	Spatial distribution of endogenous molecules	Caffeine, theophylline, theobromine, dicaffeoylquinic acid and caffeoylquinic acid	75 µm	46
Corn	TOF-SIMS-MSI	Sample preparation strategies	Fatty acid and lipids	-	47
Wheat leaf	LAESI	Study the penetration of agriculture formulations	Epoxiconazole and fluxapyroxad	-	48

1. Lorensen, M. D. B. B.; Hayat, S. Y.; Wellner, N.; Bjarnholt, N.; Janfelt, C., Leaves of Cannabis sativa and their trichomes studied by DESI and MALDI mass spectrometry imaging for their contents of cannabinoids and flavonoids. *Phytochemical Analysis* **2023,** *34* (3), 269-279.
2. Balasubramanian, V. K.; Veličković, D.; Rubio Wilhelmi, M. D. M.; Anderton, C. R.; Stewart, C. N.; DiFazio, S.; Blumwald, E.; Ahkami, A. H., Spatiotemporal metabolic responses to water deficit stress in distinct leaf cell-types of poplar. *Frontiers in Plant Science* **2024,** *15*.
3. Kazachkova, Y.; Zemach, I.; Panda, S.; Bocobza, S.; Vainer, A.; Rogachev, I.; Dong, Y.; Ben-Dor, S.; Veres, D.; Kanstrup, C.; Lambertz, S. K.; Crocoll, C.; Hu, Y.; Shani, E.; Michaeli, S.; Nour-Eldin, H. H.; Zamir, D.; Aharoni, A., The GORKY glycoalkaloid transporter is indispensable for preventing tomato bitterness. *Nature Plants* **2021,** *7* (4), 468-480.
4. Ye, H.; Gemperline, E.; Venkateshwaran, M.; Chen, R.; Delaux, P. M.; Howes-Podoll, M.; Ané, J. M.; Li, L., MALDI mass spectrometry-assisted molecular imaging of metabolites during nitrogen fixation in the M edicago truncatula–S inorhizobium meliloti symbiosis. *The Plant Journal* **2013,** *75* (1), 130-145.
5. Enomoto, H.; Sato, K.; Miyamoto, K.; Ohtsuka, A.; Yamane, H., Distribution analysis of anthocyanins, sugars, and organic acids in strawberry fruits using matrix-assisted laser desorption/ionization-imaging mass spectrometry. *Journal of Agricultural and Food Chemistry* **2018,** *66* (19), 4958-4965.
6. Dare, A. P.; Günther, C. S.; Grey, A. C.; Guo, G.; Demarais, N. J.; Cordiner, S.; McGhie, T. K.; Boldingh, H.; Hunt, M.; Deng, C., Resolving the developmental distribution patterns of polyphenols and related primary metabolites in bilberry (Vaccinium myrtillus) fruit. *Food Chemistry* **2022,** *374*, 131703.
7. Klein, A. T.; Yagnik, G. B.; Hohenstein, J. D.; Ji, Z.; Zi, J.; Reichert, M. D.; MacIntosh, G. C.; Yang, B.; Peters, R. J.; Vela, J.; Lee, Y. J., Investigation of the Chemical Interface in the Soybean–Aphid and Rice–Bacteria Interactions Using MALDI-Mass Spectrometry Imaging. *Analytical Chemistry* **2015,** *87* (10), 5294-5301.
8. Nakamura, J.; Morikawa-Ichinose, T.; Fujimura, Y.; Hayakawa, E.; Takahashi, K.; Ishii, T.; Miura, D.; Wariishi, H., Spatially resolved metabolic distribution for unraveling the physiological change and responses in tomato fruit using matrix-assisted laser desorption/ionization–mass spectrometry imaging (MALDI–MSI). *Analytical and Bioanalytical Chemistry* **2017,** *409* (6), 1697-1706.
9. Hertel Pereira, A. C.; Auer, A. C.; Biedel, L.; de Almeida, C. M.; Romão, W.; Endringer, D. C., Analysis of Gliricidia sepium Leaves by MALDI Mass Spectrometry Imaging. *Journal of the American Society for Mass Spectrometry* **2022,** *33* (3), 573-583.
10. dos Santos, N. A.; de Almeida, C. M.; Gonçalves, F. F.; Ortiz, R. S.; Kuster, R. M.; Saquetto, D.; Romão, W., Analysis of Erythroxylum coca Leaves by Imaging Mass Spectrometry (MALDI–FT–ICR IMS). *Journal of the American Society for Mass Spectrometry* **2021,** *32* (4), 946-955.
11. Vaidyanathan, S.; Fletcher, J. S.; Goodacre, R.; Lockyer, N. P.; Micklefield, J.; Vickerman, J. C., Subsurface biomolecular imaging of Streptomyces coelicolor using secondary ion mass spectrometry. *Analytical chemistry* **2008,** *80* (6), 1942-1951.
12. Cliff, J. B.; Gaspar, D. J.; Bottomley, P. J.; Myrold, D. D., Exploration of inorganic C and N assimilation by soil microbes with time-of-flight secondary ion mass spectrometry. *Applied and Environmental Microbiology* **2002,** *68* (8), 4067-4073.

13. Perkins, M. C.; Bell, G.; Briggs, D.; Davies, M. C.; Friedman, A.; Hart, C. A.; Roberts, C. J.; Rutten, F. J. M., The application of ToF-SIMS to the analysis of herbicide formulation penetration into and through leaf cuticles. *Colloids and Surfaces B: Biointerfaces* **2008,** *67* (1), 1-13.
14. Nihorimbere, V.; Cawoy, H.; Seyer, A.; Brunelle, A.; Thonart, P.; Ongena, M., Impact of rhizosphere factors on cyclic lipopeptide signature from the plant beneficial strain Bacillus amyloliquefaciens S499. *FEMS Microbiology Ecology* **2012,** *79* (1), 176-191.
15. Martin, R. R.; Naftel, S.; Macfie, S.; Skinner, W.; Courchesne, F.; Séguin, V., Time of flight secondary ion mass spectrometry studies of the distribution of metals between the soil, rhizosphere and roots of Populus tremuloides Minchx growing in forest soil. *Chemosphere* **2004,** *54* (8), 1121-1125.
16. Clode, P. L.; Kilburn, M. R.; Jones, D. L.; Stockdale, E. A.; Cliff III, J. B.; Herrmann, A. M.; Murphy, D. V., In situ mapping of nutrient uptake in the rhizosphere using nanoscale secondary ion mass spectrometry. *Plant physiology* **2009,** *151* (4), 1751-1757.
17. Behrens, S.; Lösekann, T.; Pett-Ridge, J.; Weber, P. K.; Ng, W.-O.; Stevenson, B. S.; Hutcheon, I. D.; Relman, D. A.; Spormann, A. M., Linking microbial phylogeny to metabolic activity at the single-cell level by using enhanced element labeling-catalyzed reporter deposition fluorescence in situ hybridization (EL-FISH) and NanoSIMS. *Applied and environmental microbiology* **2008,** *74* (10), 3143-3150.
18. Mandal, M. K.; Ozawa, T.; Saha, S.; Rahman, M. M.; Iwasa, M.; Shida, Y.; Nonami, H.; Hiraoka, K., Development of sheath-flow probe electrospray ionization mass spectrometry and its application to real time pesticide analysis. *Journal of agricultural and food chemistry* **2013,** *61* (33), 7889-7895.
19. Menezes, R. C.; Kai, M.; Krause, K.; Matthäus, C.; Svatoš, A.; Popp, J.; Kothe, E., Monitoring metabolites from Schizophyllum commune interacting with Hypholoma fasciculare combining LESA–HR mass spectrometry and Raman microscopy. *Analytical and Bioanalytical Chemistry* **2015,** *407* (8), 2273-2282.
20. Yamaji, N.; Ma, J. F., Bioimaging of multiple elements by high-resolution LA-ICP-MS reveals altered distribution of mineral elements in the nodes of rice mutants. *The Plant Journal* **2019,** *99* (6), 1254-1263.
21. Kötschau, A.; Büchel, G.; Einax, J.; Fischer, C.; Von Tümpling, W.; Merten, D., Mapping of macro and micro elements in the leaves of sunflower (Helianthus annuus) by Laser Ablation–ICP–MS. *Microchemical Journal* **2013,** *110*, 783-789.
22. Huang, W.; Jiao, J.; Ru, M.; Bai, Z.; Yuan, H.; Bao, Z.; Liang, Z., Localization and Speciation of Chromium in Coptis chinensis Franch. using Synchrotron Radiation X-ray Technology and Laser Ablation ICP-MS. *Scientific Reports* **2018,** *8* (1), 8603.
23. Hölscher, D.; Shroff, R.; Knop, K.; Gottschaldt, M.; Crecelius, A.; Schneider, B.; Heckel, D. G.; Schubert, U. S.; Svatoš, A., Matrix-free UV-laser desorption/ionization (LDI) mass spectrometric imaging at the single-cell level: Distribution of secondary metabolites of Arabidopsis thaliana and Hypericum species. *The Plant Journal* **2009,** *60* (5), 907-918.
24. Becker, L.; Bellow, S.; Carré, V.; Latouche, G.; Poutaraud, A.; Merdinoglu, D.; Brown, S. C.; Cerovic, Z. G.; Chaimbault, P., Correlative analysis of fluorescent phytoalexins by mass spectrometry imaging and fluorescence microscopy in grapevine leaves. *Analytical chemistry* **2017,** *89* (13), 7099-7106.
25. Taylor, M. J.; Liyu, A.; Vertes, A.; Anderton, C. R., Ambient Single-Cell Analysis and Native Tissue Imaging Using Laser-Ablation Electrospray Ionization Mass Spectrometry with Increased Spatial Resolution. *Journal of the American Society for Mass Spectrometry* **2021,** *32* (9), 2490-2494.
26. Shrestha, B.; Patt, J. M.; Vertes, A., In situ cell-by-cell imaging and analysis of small cell populations by mass spectrometry. *Analytical chemistry* **2011,** *83* (8), 2947-2955.

27. Nielen, M. W.; van Beek, T. A., Macroscopic and microscopic spatially-resolved analysis of food contaminants and constituents using laser-ablation electrospray ionization mass spectrometry imaging. *Analytical and bioanalytical chemistry* **2014,** *406* (27), 6805-6815.
28. Dong, Y.; Guella, G.; Franceschi, P., Impact of tissue surface properties on the desorption electrospray ionization imaging of organic acids in grapevine stem. *Rapid Communications in Mass Spectrometry* **2016,** *30* (6), 711-718.
29. Hartmanova, L.; Ranc, V.; Papouskova, B.; Bednar, P.; Havlicek, V.; Lemr, K., Fast profiling of anthocyanins in wine by desorption nano-electrospray ionization mass spectrometry. *Journal of chromatography A* **2010,** *1217* (25), 4223-4228.
30. Tata, A.; Perez, C. J.; Hamid, T. S.; Bayfield, M. A.; Ifa, D. R., Analysis of metabolic changes in plant pathosystems by imprint imaging DESI-MS. *Journal of The American Society for Mass Spectrometry* **2014,** *26* (4), 641-648.
31. Araújo, F.; Vieira, R.; Molano, E.; Máximo, H.; Dalio, R.; Vendramini, P.; Araújo, W.; Eberlin, M., Desorption electrospray ionization mass spectrometry imaging reveals chemical defense of Burkholderia seminalis against cacao pathogens. *RSC advances* **2017,** *7* (48), 29953-29958.
32. Xia, J.; Lou, G.; Zhang, L.; Huang, Y.; Yang, J.; Guo, J.; Qi, Z.; Li, Z.; Zhang, G.; Xu, S.; Song, X.; Zhang, X.; Wei, Y.; Liang, Z.; Yang, D., Unveiling the spatial distribution and molecular mechanisms of terpenoid biosynthesis in Salvia miltiorrhiza and S. grandifolia using multi-omics and DESI–MSI. *Horticulture Research* **2023,** *10* (7).
33. Gerbig, S.; Stern, G.; Brunn, H. E.; Düring, R.-A.; Spengler, B.; Schulz, S., Method development towards qualitative and semi-quantitative analysis of multiple pesticides from food surfaces and extracts by desorption electrospray ionization mass spectrometry as a preselective tool for food control. *Analytical and Bioanalytical Chemistry* **2017,** *409* (8), 2107-2117.
34. Nauta, S. P.; Huysmans, P.; Tuijthof, G. J.; Eijkel, G. B.; Poeze, M.; Siegel, T. P.; Heeren, R. M., Automated 3D Sampling and Imaging of Uneven Sample Surfaces with LA-REIMS. *Journal of the American Society for Mass Spectrometry* **2021,** *33* (1), 111-122.
35. Kokesch-Himmelreich, J.; Wittek, O.; Race, A. M.; Rakete, S.; Schlicht, C.; Busch, U.; Römpp, A., MALDI mass spectrometry imaging: From constituents in fresh food to ingredients, contaminants and additives in processed food. *Food Chem* **2022,** *385*, 132529.
36. Moreno-Pedraza, A.; Rosas-Román, I.; Garcia-Rojas, N. S.; Guillén-Alonso, H.; Ovando-Vázquez, C.; Díaz-Ramírez, D.; Cuevas-Contreras, J.; Vergara, F.; Marsch-Martínez, N.; Molina-Torres, J.; Winkler, R., Elucidating the Distribution of Plant Metabolites from Native Tissues with Laser Desorption Low-Temperature Plasma Mass Spectrometry Imaging. *Analytical Chemistry* **2019,** *91* (4), 2734-2743.
37. Wang, J.; Yang, E.; Chaurand, P.; Raghavan, V., Visualizing the distribution of strawberry plant metabolites at different maturity stages by MALDI-TOF imaging mass spectrometry. *Food Chem* **2021,** *345*, 128838.
38. Enomoto, H.; Sensu, T.; Yumoto, E.; Yokota, T.; Yamane, H., Derivatization for detection of abscisic acid and 12-oxo-phytodienoic acid using matrix-assisted laser desorption/ionization imaging mass spectrometry. *Rapid Communications in Mass Spectrometry* **2018,** *32* (17), 1565-1572.
39. Taira, S.; Tokai, M.; Kaneko, D.; Katano, H.; Kawamura-Konishi, Y., Mass Spectrometry Imaging Analysis of Location of Procymidone in Cucumber Samples. *Journal of Agricultural and Food Chemistry* **2015,** *63* (27), 6109-6112.
40. Montini, L.; Crocoll, C.; Gleadow, R. M.; Motawia, M. S.; Janfelt, C.; Bjarnholt, N., Matrix-Assisted Laser Desorption/Ionization-Mass Spectrometry Imaging of Metabolites during Sorghum Germination1 [OPEN]. *Plant Physiology* **2020,** *183* (3), 925-942.

41. Veličković, D.; Ropartz, D.; Guillon, F.; Saulnier, L.; Rogniaux, H., New insights into the structural and spatial variability of cell-wall polysaccharides during wheat grain development, as revealed through MALDI mass spectrometry imaging. *Journal of Experimental Botany* **2014,** *65* (8), 2079-2091.
42. Righetti, L.; Bhandari, D. R.; Rolli, E.; Tortorella, S.; Bruni, R.; Dall'Asta, C.; Spengler, B., Unveiling the spatial distribution of aflatoxin B1 and plant defense metabolites in maize using AP-SMALDI mass spectrometry imaging. *The Plant Journal* **2021,** *106* (1), 185-199.
43. Maia, M.; Aziz, A.; Jeandet, P.; Carré, V., Profiling and Localization of Stilbene Phytoalexins Revealed by MALDI-MSI during the Grapevine–Botrytis cinerea Interaction. *Journal of Agricultural and Food Chemistry* **2023,** *71* (42), 15569-15581.
44. Xie, P.; Chen, J.; Wu, P.; Cai, Z., Spatial Lipidomics Reveals Lipid Changes in the Cotyledon and Plumule of Mung Bean Seeds during Germination. *Journal of Agricultural and Food Chemistry* **2023,** *71* (49), 19879-19887.
45. Zhao, Y.; Jiang, M.; Liu, M.; Wang, H.; Wang, W.; Zhang, T.; Tian, X.; Hong, L.; Yang, F.; Wang, Y.; Zou, Y.; Yu, H.; Li, Z.; Yang, W., Spatial Distribution and Characterization of the Small-Molecule Metabolites and In Situ Hydrolyzed Oligosaccharides in the Rhizome of Glycyrrhiza uralensis by Desorption Electrospray Ionization-Mass Spectrometry Imaging and High-Resolution Liquid Chromatography–Mass Spectrometry. *Journal of Agricultural and Food Chemistry* **2023,** *71* (50), 20372-20385.
46. Li, N.; Dong, J.; Dong, C.; Han, Y.; Liu, H.; Du, F.; Nie, H., Spatial Distribution of Endogenous Molecules in Coffee Beans by Atmospheric Pressure Matrix-Assisted Laser Desorption/Ionization Mass Spectrometry Imaging. *Journal of the American Society for Mass Spectrometry* **2020,** *31* (12), 2503-2510.
47. Kim, S. H.; Kim, J.; Lee, Y. J.; Lee, T. G.; Yoon, S., Sample Preparation of Corn Seed Tissue to Prevent Analyte Relocations for Mass Spectrometry Imaging. *Journal of The American Society for Mass Spectrometry* **2017,** *28* (8), 1729-1732.
48. Annangudi, S. P.; Gemperline, E.; Gilbert, J. R., Spatial and Depth Profiling of Agricultural Formulations in Leaf Tissue Using LAESI Mass Spectrometry. *Journal of the American Society for Mass Spectrometry* **2024,** *35* (5), 1007-1011.